IJE TRANSACTIONS C: Aspects Vol. 35 No. 12, (December 2022) 2350-2358

International Journal of Engineering

Journal Homepage: www.ije.ir

# Effects of Inflation Pressure and Wall Thickness on Gripping Force of Semi-Cylindrical Shaped Soft Actuator: Numerical Investigation

D. Doreswamy[a], S. S. Menon[a], J. M. D'Souza[a], S. K. Bhat*[b]

[a] *Department of Mechatronics, Manipal Institute of Technology, Manipal Academy of Higher Education, Manipal, Karnataka, India*
[b] *Department of Mechanical and Manufacturing Engineering, Manipal Institute of Technology, Manipal Academy of Higher Education, Manipal, Karnataka, India*

*P A P E R   I N F O*

*Paper history:*
Received 17 August 2022
Received in revised form 08 September 2022
Accepted 16 September 2022

*Keywords*:
*Soft Actuator*
*Pneu-Net*
*Hyperelasticity*
*Inflation Pressure*
*Gripping Force*

*A B S T R A C T*

Soft robotics using Pneumatic Network actuators (Pneu-Net) is a developing field that has a promising future for variety of applications involving delicate operations such as biomedical assistance. The interaction between geometry and the performance of the actuator is an important topic which has been studied by many researchers in this field. However, there is a lack of investigation on the relationship between gripping capability and geometrical parameters of soft actuators. Especially, there is a need to shed more light on the effects of wall thicknesses on the gripping force developed. In the present study, a semi-cylindrical chambered PneuNet soft actuator is numerically investigated to evaluate the effects of pressure and wall thickness variations on its performance characteristics. The results revealed that increasing the restraining layer thickness (RLT) aids the bending capability of the actuator whereas increasing the chamber wall thickness reduces it. Therefore, maximum bending of the actuator is achieved at the combinations of minimum wall thickness and maximum RLT. At these geometrical configurations of maximum bending, the deformation-pressure relationships followed a sigmoidal function and tended towards linearity with increasing wall thickness and decreasing RLT. The gripping force showed an exponential increase with increasing working pressures and wall thicknesses. The maximum gripping force increased cubically with increasing wall thicknesses at their respective maximum working pressures, which was modeled using a polynomial regression model ($R^2$=99.79%).

***doi**: 10.5829/ije.2022.35.12c.11*

## 1. INTRODUCTION

Robotics is a vast area that caters to various domains and applications including automobile engineering, biomedical engineering, and so on. Conventionally, the robots are made up of rigid materials which are suited for handling hard materials. These robots can be used to perform robust and intensive tasks. However, they are not applicable for tasks that require a soft and feather touch or need to interact with delicate organisms or objects in their workspace. Such gentle tasks can be taken up by robots made up of soft, rubber-like materials. A wide array of applications is possible for such robots, such as medical and exploration fields where the traditional robots cannot be easily employed because of the rigid connections and joints that they are made up of. Also, soft robots can be applied to work alongside humans without causing any harm to those working in proximity. For instance, honeycomb structures can provide a larger deformation with a relatively lesser quantity of material. Further, different types of materials can be utilized according to the load carrying capability and usability criteria of the soft robots. It is observed that there are various methods of actuation that can be used in accordance with the use case and the materials used [1].

Soft robotics can be utilized for various biomedical applications, and can assist in sensitive and intricate surgical procedures while reducing the human induced errors [2]. Wearable soft robots can be developed to aid in the rehabilitation process providing a much better

*Corresponding Author Institutional Email: sk.bhat@manipal.edu (S. K. Bhat)

Please cite this article as: D. Doreswamy, S. S. Menon, J. M. D'Souza, S. K. Bhat, Numerical Investigation on A Novel Curling Semi-Cylindrical Soft Pneumatic Actuator: The Effects of Inflation Pressure and Wall Thickness on The Gripping Force, ***International Journal of Engineering, Transactions C: Aspects***, Vol. 35, No. 12, (2022), 2350-2358

recovery rate and long-term usage. A wide variety of soft actuators have been developed for biomedical applications [3]. Soft robots that mimic human organs need to be made of compliant materials which respond to natural stimuli [2]. Various combinations of materials and actuation methods can be used to solve certain types of use cases. Apart from the complex applications such as mimicking human organs and animal motions, soft robots can also perform picking and placing operations. Zheng et al. [4] developed a soft robot inspired by the water animal, Ascidian, capable of performing pick-and-place operations such as drug-release tasks in millimeter scale. Such robots can be used for exploration and interaction with different organisms. Several gripping technologies exist which can be used for simple cases [5]. It is observed that the most common method of actuation is by application of air or fluidic pressure in the internal chambers of the actuators, which are known as Pneumatic Networks or PneuNets [6]. The major point of focus of the present study is to develop a gripper using soft materials that be used to pick-and-place sensitive objects without damaging them.

One of the most fascinating use cases of Pneumatic Networks is the creation of rehabilitation gloves that are used for fine movements of the hands during physiotherapy after a serious injury. It is observed that the use of soft robots provides a more comfortable and quicker recovery than the traditional rigid methods. The finger-like structure consists of internal chambers that can be filled with fluid or air. As the fluidic pressure increases through the tubular structures, the finger-like structure begins to bend, aiding in the bending of the human hands of the user undergoing physiotherapy. This type of therapy is used to regain the lost motion of fingers after serious injuries. Numerous grippers are being tested and compiled to obtain the required characteristics with a large variety of possible actuations [5]. Pneumatically operated grippers have been explored for industrial applications to increase productivity of transporting operations [7-9]. Researchers have developed advanced control systems and machine learning based tools for biomedical applications and for enhancing the learning process of students in educational institutes [10,11].

Numerous materials can be used to create soft robots as explained in works conducted by Rossiter et al. [12], Shen et al. [13], Manti et al. [14] and Wu et al. [15]. The actuation methods can be modified based on material properties as discussed by Hughes et al. [16] and Bira et al. [17]. The materials used can define the use case and the limits of the robot. This has been realized and optimized in the works introduced by Mosadegh et al. [18] and Yan et al. [19]. The most common materials used for PneuNet based soft grippers are usually elastomers and they have a wide range of applications as seen in research conducted by Zhou and Li [20], Liu et al. [21]. For simulations and analyses, these materials are considered as hyperelastic materials. Hyperelastic materials exhibit nonlinear stress-strain relationships and tend to retain their shape after the removal of external forces and can undergo numerous loading and unloading cycles without undergoing plastic deformation.

The structure of the actuator chamber plays an important role on the nature of deformations exhibited in literature [7,22,23]. The major mode of actuation that is being developed and in focus for actuation in the present paper is the pneumatic network with reference to works conducted by Honarpardaz [24]. These consist of multiple pneumatic chambers that can be in series or parallel connection to each other. On application of pneumatic pressure in these chambers, it expands applying pressure on the restraining layer causes a bending motion, which is used to actuate and carry out the gripping mechanism. The restraining layer can consist of a different material or can be implemented by increasing the thickness of the layer [25]. The absence of this restraining layer causes the actuator to expand radially and laterally without undergoing bending. The geometry and the size of the internal pneumatic chamber define the bending and gripping force of the developed gripper [26]. Also, the direction of expansion is majorly defined by the geometry of the individual chambers.

From the literature review on geometrical aspects of soft actuators it is observed that, comparatively fewer studies have investigated the semi-cylindrical shaped actuators [27-30]. Among these studies, Tan et al. [28] and Wang et al. [30] experimentally measured the forces generated by the soft gripppers. However, as per the best information of the authors, the effects of restraining layer thicknesses on the gripping force generation has not been investigated. In this perspective, the gripping force and deformation characteristics of soft actuators can be modified by varying the wall thicknesses and the pneumatic actuation pressure. Thus, the present study focused on the numerical investigation of a semi-cylindrical silicone-based soft actuator by varying each parameter individually while keeping the remaining parameters constant to understand the effect of the corresponding parameter on its deformation characteristics. Based on the results obtained with the variations of the parameters, a suitable configuration of the parameters can be chosen depending on the application where the soft robot is being employed. Further, the working pressure for such robots and the critical pressure above which they may malfunction can also be determined. Thus, the present study aims to arrive at a comprehensive understanding of the characteristics of a semi-cylindrical silicone-based soft actuator. Based on these results, a suitable actuator can then be developed in a robust and systematic manner according to the deformation characteristics and the gripping force requirements of specific applications.

## 2. MATERIALS AND METHODS

**2. 1. Hyperelastic Material Model** For the simulation and analysis of the soft robotics structures, the materials are considered as hyperelastic in nature. These materials deform and later with the removal of the pressure return to their original shape, i.e., they do not undergo any plastic deformation. They can undergo such deformation cycles numerous times without undergoing permanent deformations. Various hyperelastic material models can be used to predict the stress-strain curve closely to the original curve [31]. Selection of a hyperelastic model involves a choice between complexity of models with higher number of material parameters which help in precise fitting to experimental data and on the other hand simple models with stable and acceptable results with reasonable accuracy. Compared to other models, Yeoh model is found to be efficient in this regard because of its simplicity, smaller number of material parameters and ability to describe multi-axial deformation behaviors [32]. In the present study, the 2nd order Yeoh hyperelastic model was used for the simulations [33] as shown in Equation (1).

$$W = \sum_{i=1}^{2} C_i (I_1 - 3)^i + D[compression\ term] \quad (1)$$

where, $W$ is the strain-energy potential, $I_1$ is the first invariant of the right Cauchy-Green deformation tensor, and $C_i$ are the material constants. By assuming incompressibility of the material, the compression term is taken to be null. The order of series expansion can be done based on the number of terms required to represent the experimental deformation characteristics. The material constants of the Yeoh 2nd order model used in the present numerical investigation with the constant values stated in Table 1 [34]. Using the strain-energy expression of Equation (1), the stress-strain relationship under uniaxial loading can be obtained as follows [30].

$$\sigma = \sum_{i=1}^{n} 2C_i \cdot i \cdot (\lambda - \lambda^{-2}) \cdot (\lambda^2 + 2\lambda^{-1} - 3)^{i-1} \quad (2)$$

where, σ is the Cauchy stress developed, λ is the ratio of deformed length to actual length (1+nominal strain). By substituting the constants in Table 1 in Equation (2), a graph of stress vs strain is plotted (Figure 1). It is observed that with an increase in strain, the rate at which the stress is developed increases.

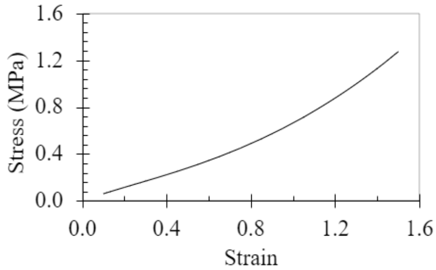


**Figure 1.** Stress-strain relationship with the Yeoh model

**TABLE 1.** Material constants of Yeoh model [29]

| Constant | Values (MPa) |
|---|---|
| $C_1$ | 0.11 |
| $C_2$ | 0.02 |
| D | 0 |

**2. 2. Modeling of the Computational Domain and Boundary Conditions** As discussed in the Introduction, actuator geometries govern the nature of deformation exhibited the actuators. The "semi-cylinder chamber" type of actuator was chosen for the present study (Figure 2) because of its tendency to curl and bend under the action of pressure through its chambers. The gripping action aimed to be obtained is achieved by curling around an object. The boundary conditions applied are shown in Figure 2. The actuator is considered to be fixed at one end and free at the other end. A static pressure is applied on all the internal faces of the chambers, which is varied between 100 kPa and 350 kPa in the analyses (Figure 2).

Figure 3 shows the details of the geometrical parameters which were varied during the analysis, i.e., the restraining layer thickness (RLT) and wall thickness ((D-d)/2). The total length of the gripper unit (L) measured between the inner faces is kept constant at 150 mm. Table 2 presents the different combinations of dimensions that were considered. The outer radius (D/2) of the structure varies from 8.5 mm to 11.5 mm with a gradual increase of 1 mm. It is observed that with an increase in the wall thickness, the gaps decrease as the total length of the internal chamber remains constant.

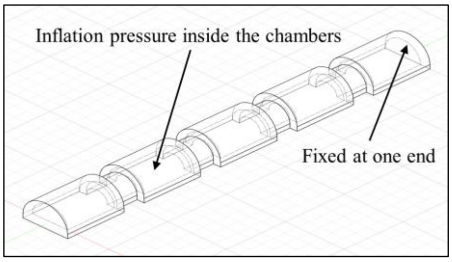


**Figure 2.** Boundary conditions on the semi-cylindrical actuator gripping unit

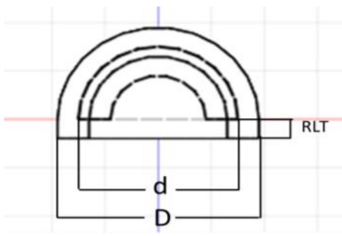


**Figure 3.** Geometrical parameters varied in the analysis

**TABLE 2.** Parametric variations of the dimensions (mm)

| Sl. no. | L | RLT | d/2 | D/2 | (D-d)/2 |
|---|---|---|---|---|---|
| 1 | 150 | 5 | 7.5 | 8.5 | 2 |
| 2 | 150 | 5 | 7.5 | 9.5 | 3 |
| 3 | 150 | 5 | 7.5 | 10.5 | 4 |
| 4 | 150 | 5 | 7.5 | 11.5 | 5 |
| 5 | 150 | 2.5 | 7.5 | 10 | 2.5 |
| 6 | 150 | 5 | 7.5 | 10 | 2.5 |
| 7 | 150 | 7.5 | 7.5 | 10 | 2.5 |

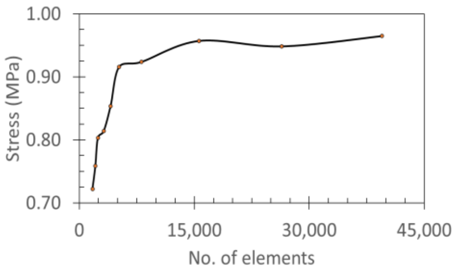


**Figure 4.** No. of elements vs stress developed

**2. 3. Grid-Independence Study** The computational domain is discretized using second-order tetrahedral elements. To identify the optimum size of the elements for the numerical analyses, the grid-independence study is conducted. For this purpose, the numerical model is simulated at a pressure of 100 kPa while the element size is varied until a result is obtained which is independent of further refinement of mesh sizing. It is observed from Figure 4 that the results do not show significant difference above 15,000 elements. Thus, the element size for this case, i.e., 0.15 mm was chosen for further numerical analyses which was found to be the optimum mesh size for obtaining satisfactory results.

**2. 4. Gripping Force Evaluation** The gripping force has to be modulated based on the required application as discussed by Wang et al. [36, 37] and Cacucciolo et al. [38]. The bending of the actuator is postulated to be along the side of the restrain layer [39]. On application of the inflating pressure, the gripping actuator unit undergoes deformation. For this end, the gripping actuator unit (placed on top of the rigid block, shown in Figure 5) is placed on a solid, rigid block made up of structural steel (Figure 5), and the inflating pressure is applied on the actuator. The force generated by the actuator's bottom surface is measured as the resultant reaction force developed at the bottom surface of the rigid block. A methodology (Figure 6) has been proposed in this study to measure the gripping force which is generated by the gripping unit.

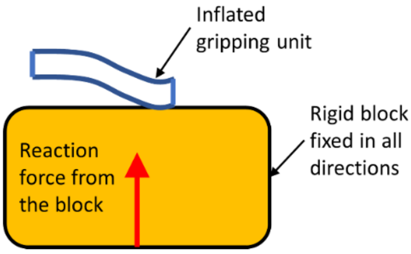


**Figure 5.** Schematic of FEA for gripping force evaluation

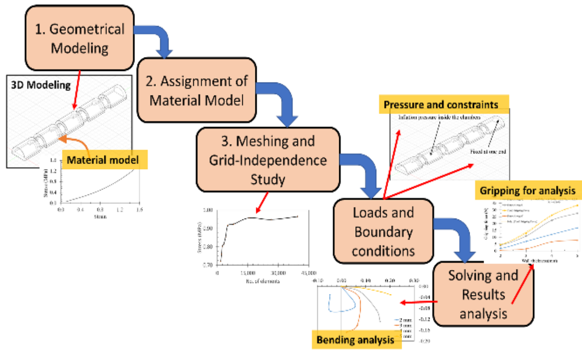


**Figure 6.** Research methodology of the present study

## 3. RESULTS AND DISCUSSION

**3. 1. Effect of Pressure on Deformation of The Actuator** Pneumatic networks operate by deforming on the application of different values of internal pressures. It can be postulated that on increasing the internal pressure the deformation of the structure increases. However, wall thickness and RLT play a key role in deciding the extent and nature of deformation observed. Figures 7(a) and 7(b) show the variations of bending profiles of the actuator with changes in wall thickness and RLT, respectively. It is observed that increasing RLT leads to increased bending whereas increasing the wall thickness leads to reduction in the bending of the actuator. This is because, wall thickness increases the rigidity of the layer; thereby reducing the amount of bending. Thus, a higher RLT and lower wall thickness is advisable for the required gripping mode of the actuator.

Figures 8(a) and 8(b) show the changes in total deformation of the actuator with increase in inflating pressures. In case of variation of wall thickness, the relationship between maximum deformation and pressure is inversely proportional. Thus, it can be inferred that with an increase in the wall thickness the total deformation values decrease proportionally. It is also noted that an increase in wall thickness decreases the nonlinearity of the deformation-pressure relationship. Notably, at 2 mm wall thickness, the total deformation variation follows a sigmoidal curve, and with an increase

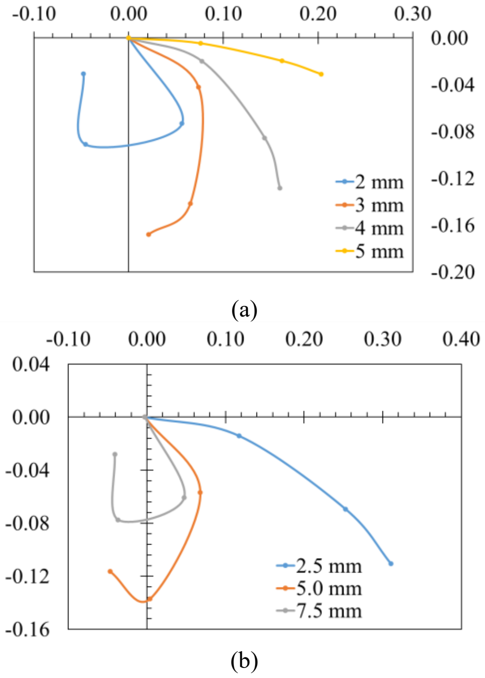


**Figure 7.** Bending profiles for varying (a) wall thickness and (b) RLT

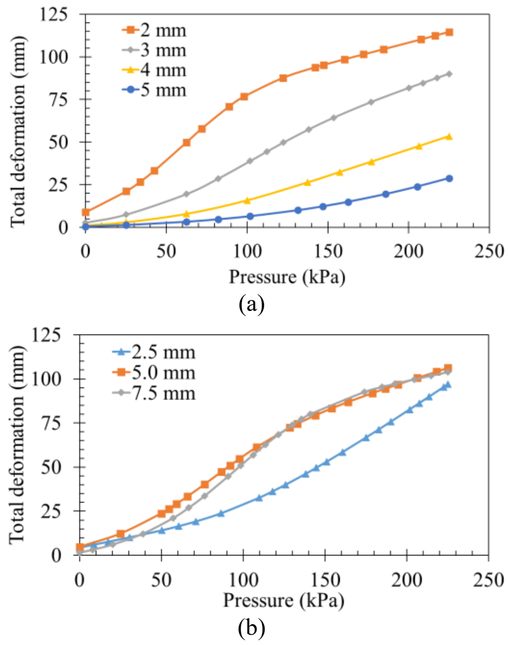


**Figure 8.** Total deformation results for variations of (a) wall thickness and (b) RLT

in the thickness, the curve becomes closer to a linear profile. Thus, it can be deduced that with higher wall thicknesses, the geometry becomes bulky leading to increase in the effect of geometry of the structure compared to the effect of material nonlinearity of the soft material.

With an increase in RLT, the total deformation increased until the RLT of 7.5 mm. However, this result does not provide a complete description of its deformation behavior. It is observed that an increase in RLT results in increased bending whereas an increase in wall thickness leads to an increase in radial expansion of the gripping unit. Therefore, to attain the curling motion for the gripping actuation, radial expansions and longitudinal expansions have to be minimized and bending actuation should be maximized. Notably, at 5 and 7.5 mm RLT, the total deformation variation follows a sigmoidal curve, and with a decrease in RLT, the nonlinearity of the deformation-pressure curve decreases. As RLT reduces, the effect of expanding flexible wall increases which augments the effect of the nonlinear nature of the material to the forefront by reducing the bulkiness of the geometrical structure.

## 3. 2. Effect of Pressure on Strain Variations

With the increase in the internal pressure the actuator is made to expand, resulting in a change in strain values. The internal pressure is increased from 0 kPa to 225 kPa in a quasi-static manner. For various pressure levels, strain values were recorded and plotted as shown in Figures 9(a) and 8(b). Since, strain is an absolute quantity normalized with respect to the initial dimension of an object, in both the cases of an increase in wall thickness and RLT, it is observed that strain decreases with addition of material. This is because, with the addition of material the average stiffness of the actuator increases; thereby reducing the average strains. Our analysis revealed that the average stresses also follow a similar tendency as average strains.

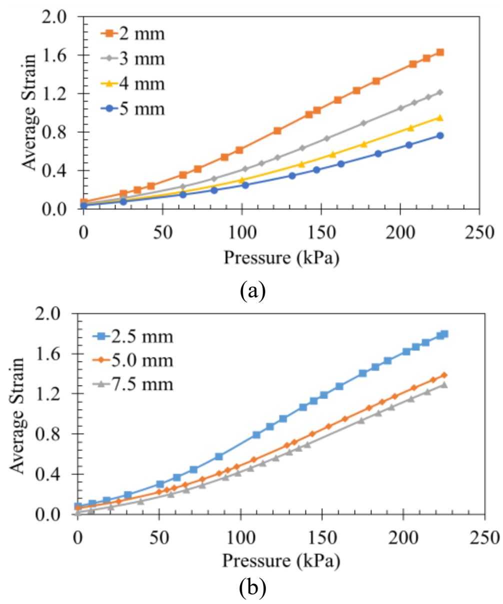


**Figure 9.** Effect of pressure on average strain for variations of (a) wall thickness and (b) RLT

### 3. 3. Effects of Pressure and Thickness on the Gripping Force Developed by the Actuator

Figure 10(a) shows the effect on gripping force as the chamber wall thickness increases while keeping a constant base layer thickness (RLT) of 5mm. From the obtained results it can concluded that with an increase in wall thickness, higher working internal pressure can be employed for the gripping actuation, leading to higher gripping forces. The gripping force tends to follow an exponential law, increasing with the increase in working internal gripping force and wall thickness. The maximum gripping force achieved in the simulations were around 35 N at 300 kPa pressure for 5 mm thick RLT. In an experimental study of human thumb inspired semi-cylindrically shaped soft actuator, Wang et al. [30] reported a comparable gripping force between 30 N – 40 N having a nonlinear variation with respect to actuation pressure as observed in Figure 9(a). Although the shapes of their internal chamber were different, the forces were in the same order as in the present study. Further, Chatterjee et al. [40] fabricated a human finger inspired actuator in the shape of a hollow semi-cylindrical tube, in which they observed a force generation of around 1.2 N at an actuation pressure of 30 kPa, which is again in the range of results in the present paper at the same pressure level.

For a better understanding of the effect of wall thicknesses, the force values are evaluated at a common pressure of 100 kPa and RLT of 5 mm and depicted as shown in Figure 10b. From this result it is noted that with an increase in wall thickness from 2 mm to 5 mm, the gripping force increases and becomes saturated at 5 mm thickness. This saturation can be accounted for by an increase in the pressure requirements for actuation with increased wall thicknesses. As wall thickness increases, the pressure applied, i.e., 100 kPa, is comparatively low to produce higher gripping forces. Since, an actuator with higher thickness can bear higher pressures, it develops higher gripping forces as depicted in Figure 9(a).

Figure 10(c) illustrates the maximum gripping force developed by the gripping unit by curling around it at their maximum bearable internal pressures. Force vector components along the three major axes, X, Y, and Z, are plotted. The effective gripping force developed by the actuator has been plotted and a regression equation is developed. The developed cubic polynomial regression model has an $R^2$ value of 99.79%. It is observed that with an increase in wall thicknesses, the working pressure and maximum gripping force increases nonlinearly. This variation of the gripping force tends to follow a sigmoidal nature of curve. Similar trends of the nonlinear gripping force variations (sigmoidal variation) has been observed in the study conducted by Wang et al. [30].

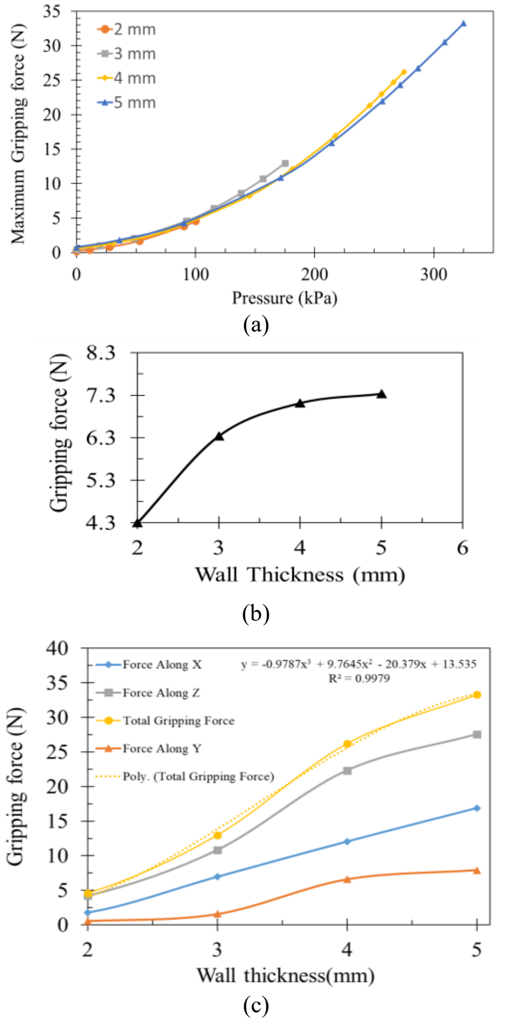


**Figure 10.** Gripping force variations with (a) varying pressures and wall thicknesses, (b) constant pressure of 100 kPa and (c) different wall thicknesses and corresponding maximum working pressures

### 3. 4. Effects of Geometric Parametric Variations on Maximum Stresses and Strains

Two types of parametric variations in the geometrical dimensions were considered for the present paper while keeping the remaining dimensional details constant. The geometry that is considered is a semi-cylindrical internal chamber. The flat part of the geometry is considered the restraining or base layer. The thickness of this layer is varied from 2.5 mm to 7.5 mm with an increment of 2.5 mm, by keeping the chamber wall thickness constant at 2.5 mm. The second type of geometrical variations considered is by keeping the base layer or restrain layer constant at 5 mm and varying the chamber wall thickness from 2 mm to 5 mm with an increment of 1 mm. The working internal pressures considered during these parametric variations were different to understand the effect of actuation pressure on the deformation characteristics. To further understand the effects of the parametric variations on the strain and stress states of the actuator, Figures 10 and 11, respectively, are shown. The Figures 11 and 12 are plotted at constant pressures of 225 kPa and 150 kPa, respectively.

Chamber wall thickness and RLT are the key factors that affect the stress developed. Figure 11 shows the relationships between the chamber wall thickness and RLT with maximum stresses developed in the actuator.

As the thicknesses increase the stress developed by the model decreases at a constant pressure. However, it needs to be noted that with increasing thicknesses, the working pressure of the actuator increases thereby increasing actual maximum pressures experienced by the actuators during their operations. As postulated earlier in case of Figure 8, the stresses and strains follow a declining trend with increase in the thickness of the material.

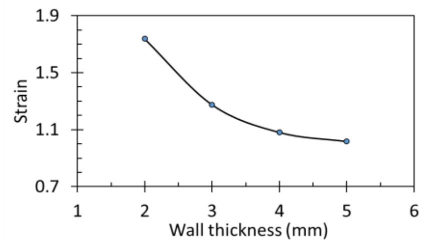


(a)

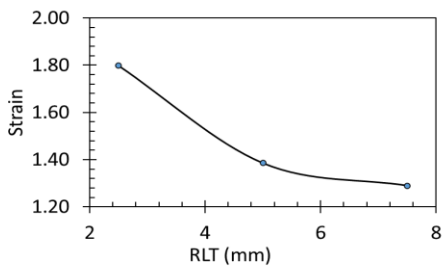


(b)

**Figure 11.** Effect of variations in (a) wall thickness and (b) RLT on maximum strain developed in the actuator

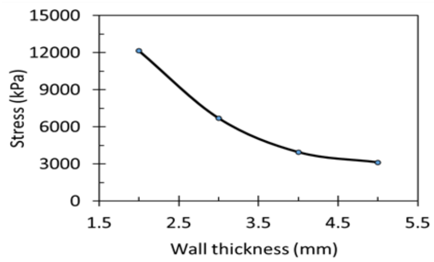


(a)

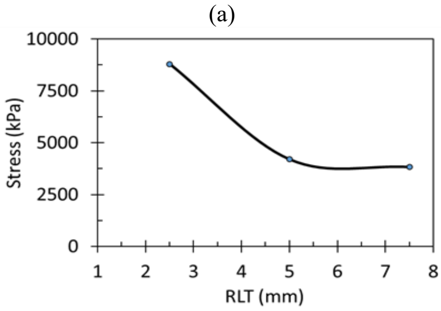


(b)

**Figure 12.** Effect of variations in (a) wall thickness and (b) RLT on maximum stresses developed in the actuator

From the effects of geometric parametric variations, it can be observed that the maximum stresses and strains developed on the chamber walls and restraining layer thickness increases with increasing working pressures. Thus, using thinner walls or restraining layers will result in more portable gripping units that require less working pressure to attain the same deformation. However, the RLT has a positive effect on the bending capability of the actuator as shown in Figure 7. Thus, a tradeoff has to be made between RLT and the stresses the actuator may be subjected to during its working conditions. The developed actuator has potential applications such as smart harvesting of delicate agricultural produce (such as tomatoes) [40, 41] and biomedical assistance to the elderly [42-44].

The present study does have certain limitations. Since, in the current work, the effect of dynamic loading scenarios have not been simulated and the focus was only on static response of the actuator, the inertial effects (effect of gravity) has not been considered in the analysis. The effect of friction between the object and the grabber has not been considered in the present analyses. This will lead to underestimation of the gripping forces developed. Hence, this is a scope for future work.

## 4. CONCLUSIONS

The numerical analysis of the novel curling semi-cylindrical actuator revealed its capability to curl into a complete 360° and thus producing a robust gripping force distribution for holding delicate objects with precision. Based on the study on the effects of pressure and thickness variations on the performance of semi-cylindrical pneumatic soft actuator, the following conclusions are drawn:

- Increasing wall thickness leads to increased radial expansion and decreased bending whereas increasing the RLT increases the bending capability of the actuator. Complete curling of the actuator is achieved for two combinations of wall thickness and RLT: (2 mm, 5 mm) and (2.5 mm and 7.5 mm), respectively.
- The deformation-pressure relationship at 2 mm wall thickness and 5 mm RLT follow a sigmoidal curve and with increasing wall thicknesses the nonlinearity decreases. With decreasing RLT from 5 mm to 2.5 mm the deformation-pressure relationship become close to a linear function.

- The gripping force increases exponentially with an increase in applied pressure as well as both wall thickness and RLT due to the increase in working pressure capability with increasing thicknesses.
- For a common actuating pressure, the gripping force is seen to saturate at a certain thickness, while for the maximum working pressure the gripping force increases nonlinearly. A third-order polynomial model is developed to represent the relationship between wall thickness and total gripping force developed at the maximum operating pressures, which showed an $R^2$=99.79%, valid for the range: 2 mm ≤ wall thickness ≤ 5 mm and 2.5 mm ≤ RLT ≤ 7.5 mm.

## 5. ACKNOWLEDGEMENT

We thank Manipal Institute of Technology, Manipal Academy of Higher Education for providing the necessary facilities for carrying out this project.

## 6. REFERENCES

1. El-Atab, N., Mishra, R.B., Al-Modaf, F., Joharji, L., Alsharif, A.A., Alamoudi, H., Diaz, M., Qaiser, N. and Hussain M.M. "Soft Actuators for Soft Robotic Applications: A Review" ***Advanced Intelligent Systems***, Vol. 2, (2020), 2000128. doi: 10.1002/aisy.202000128
2. Cianchetti, M., Laschi, C., Menciassi, A. and Dario, P. "Biomedical applications of soft robotics" ***Nature Reviews Materials***, Vol. 3, (2018), 143-153. doi: 10.1038/s41578-018-0022-y
3. Hsiao, J., Chang, J-Y. and Cheng, C.M. "Soft medical robotics: clinical and biomedical applications, challenges, and future directions" ***Advanced Robotics***, Vol. 33, No. 21, (2019), 1099-1111. doi: 10.1080/01691864.2019.1679251
4. Zheng, S., Park, T., Hoang, M.C., Go, G., Kim, C-S., Park, J-O., Choi, E. and Hong A. "Ascidian-Inspired Soft Robots That Can Crawl, Tumble, and Pick-and-Place Objects" ***IEEE Robotics and Automation Letters***, Vol. 6, No. 2, (2021), 1722-1728. doi: 10.1109/LRA.2021.3059621
5. Terrile, S., Argüelles, M. and Barrientos, A. "Comparison of Different Technologies for Soft Robotics Grippers" ***Sensors***, Vol. 21, (2021), 3253. https://doi.org/10.3390/s21093253
6. Wang, J., Fei, Y. and Pang, W. "Design, Modeling, and Testing of a Soft Pneumatic Glove with Segmented PneuNets Bending Actuators" ***IEEE/ASME Transactions on Mechatronics***, Vol. 24, No. 3, (2019), 990-1001. doi: 10.1109/TMECH.2019.2911992
7. Savkiv, V., Mykhailyshyn, R., Duchon, F., Prentkovskis, O., Maruschak, P. and Diahovchenko, I. "Analysis of Operational Characteristics of Pneumatic Device of Industrial Robot for Gripping and Control of Parameters of Objects of Manipulation." ***Transbaltica XI: Transportation Science and Technology***, Transbaltica 2019. Lecture Notes in Intelligent Transportation and Infrastructure. Springer, (2020). 504-510. doi: 10.1007/978-3-030-38666-5_53
8. Savkiv, V., Mykhailyshyn, R., Duchon, F. and Maruschak, P. "Justification of Influence of the Form of Nozzle and Active Surface of Bernoulli Gripping Devices on Its Operational Characteristics" ***Transbaltica XI: Transportation Science and Technology***, Transbaltica 2019. Lecture Notes in Intelligent Transportation and Infrastructure. Springer, (2020). 263-272. doi: 10.1007/978-3-030-38666-5_28
9. Savkiv, V., Mykhailyshyn, Maruschak, P., Kyrylovych, V., Duchon, F. and Chovanec, L. "Gripping Devices of Industrial Robots for Manipulating Offset Dish Antenna Billets and Controlling Their Shape" ***Transport***, Vol. 36, No. 1, (2021), 63-74. doi: 10.3846/transport.2021.14622
10. Poolsawad, K., Songkram, N., Piromsopa, K. and Songkram, N. "Teachers' Perception for Integrating Educational Robots and Use as Teaching Assistants in Thai Primary Schools" ***Emerging Science Journal***, Vol. 4, (2020), 127-140. doi: 10.28991/esj-2021-SP1-09
11. Iswanto, I., Ma'arif, A., Raharja, N.M., Hariadi, T.K. and Shomad, M.A. "Using a Combination of PID Control and Kalman Filter to Design of IoT-based Telepresence Self-balancing Robots during COVID-19 Pandemic" ***Emerging Science Journal***, Vol. 4, (2020), 241-261. doi: 10.28991/esj-2021-SP1-016
12. Rossiter, J., Walters, P. and Stoimenov, B. "Printing 3D dielectric elastomer actuators for soft robotics" In Electroactive Polymer Actuators and Devices (EAPAD) 2009, 7287, (2009). https://doi.org/10.1117/12.815746
13. Shen, Z., Chen, F., Zhu, X., Yong, K-T. and Gu, G. "Stimuli-responsive functional materials for soft robotics" ***Journal of Materials Chemistry B***, Vol. 8, (2020), 8972-8991. doi: 10.1039/D0TB01585G
14. Manti, M., Hassan, T., Passetti, G. and D'Elia, N., Laschi, C., Cianchetti M. "A Bioinspired Soft Robotic Gripper for Adaptable and Effective Grasping" ***Soft Robotics***, Vol. 2, No. 3, (2015), 107-116. doi: 10.1089/soro.2015.0009
15. Wu, S., Hu, W., Ze, Q., Sitti, M. and Zhao, R. "Multifunctional magnetic soft composites: a review" ***Multifunctional Materials***, Vol. 3, (2020), 042003. doi: 10.1088/2399-7532/abcb0c
16. Hughes, J., Culha, U., Giardina, F., Guenther, F., Rosendo, A. and Iida, F. "Soft Manipulators and Grippers: A Review" ***Frontiers in Robotics and AI***, Vol. 3, (2016), 69. doi: 10.3389/frobt.2016.00069
17. Bira, N., Dhagat, P. and Davidson J.R. "A Review of Magnetic Elastomers and Their Role in Soft Robotics" ***Frontiers in Robotics and AI***, Vol. 7, (2020), 588391. doi: 10.3389/frobt.2020.588391
18. Mosadegh B., Polygerinos, P., Keplinger, C., Wannstedt, S., Shepherd, R.F., Gupta, U., Shim, J., Bertoldi, K., Walsh, C.J. and Whitesides G.M. "Pneumatic Networks for Soft Robotics that Actuate Rapidly" ***Advanced Functional Materials***, Vol. 24, (2014), 2163-2170; doi: 10.1002/adfm.201303288
19. Yan J., Zhang, X., Xu, B. and Zhao J. "Pneumatic Networks for Soft Robotics that Actuate Rapidly." ***Soft Robotics***, Vol. 5, No. 5, (2017), 2163-2170. doi: 10.1089/soro.2017.0040
20. Zhou, W. and Li, Y. "Modeling and Analysis of Soft Pneumatic Actuator with Symmetrical Chambers Used for Bionic robotic Fish." ***Soft Robotics***, Vol. 7, No. 2, (2018), 168-178. DOI: 10.1089/soro.2018.0087
21. Liu, X., Zhao, Y., Geng, D., Chen, S., Tan, X. and Cao C. "Soft Humanoid Hands with Large Grasping Force Enabled by Flexible Hybrid Pneumatic Actuators." ***Soft Robotics***, Vol. 8, No. 2, (2020), 175-185. doi: 10.1089/soro.2020.0001
22. Chandler, J.H., Chauhan, M., Garbin, N., Obstein, K. and Valdastri, P. "Parallel Helix Actuators for Soft Robotic Applications." ***Frontiers in Robotics and AI***, Vol. 7, (2020), 119. doi: 10.3389/frobt.2020.00119
23. Zhang J., Wang, T., Wang J., Wang, M.Y., Li B., Zhang, X.J. and Hong, J. "Geometric Confined Pneumatic Soft–Rigid Hybrid

Actuators" ***Soft Robotics***, Vol. 7, No. 5, (2018), 574-582. doi: 10.1089/soro.2018.0157

24. Honarpardaz, M. "A methodology for design and simulation of soft grippers" ***Simulation***, Vol. 97, No. 11, (2021), 779-791. doi: 10.1177/00375497211018743
25. Jing, X., Chen, S., Zhang, C. and Xie, F. "Increasing Bending Performance of Soft Actuator by Silicon Rubbers of Multiple Hardness" ***Machines***, Vol. 10, (2022), 272. doi: 10.3390/machines10040272
26. Zhou, X., Majidi, C. and O'Reilly, O.M. "Soft hands: An analysis of some gripping mechanisms in soft robot design" ***International Journal of Solids and Structures***, Vol. 64-65, (2015), 155-165. doi: 10.1016/j.ijsolstr.2015.03.021
27. Luo, M., Tao, W., Chen, F., Khuu, T.K., Ozel, S. and Onal, C.D. "Design improvements and dynamic characterization on fluidic elastomer actuators for a soft robotic snake" 2014 IEEE International Conference on Technologies for Practical Robot Applications, (2014), 1-16. doi: 10.1109/TePRA.2014.6869154
28. Tan, N., Gu, X. and Ren, H. "Design, characterization and applications of a novel soft actuator driven by flexible shafts" ***Mechanism and Machine Theory***, Vol. 122, (2018), 197-218. doi: 10.1016/j.mechmachtheory.2017.12.021
29. Pranav, V.K., Prakash, A., Rajendran, A. and Sreedharan, P. "Design optimization and analysis of external corrugation and geometry of asymmetrical bellow flexible pneumatic actuator" ***IOP Conf. Series: Materials Science and Engineering***, Vol. 1132, (2021), 012011. doi: 10.1088/1757-899X/1132/1/012011
30. Wang, Y., Kokubu, S., Zhou, Z., Guo, X., Hsueh, Y.H. and Yu, W. "Designing soft pneumatic actuators for thumb movements" ***IEEE Robotics and Automation Letters***, Vol. 6, No. 4, (2021), 8450-8457. doi: 10.1109/LRA.2021.3105799
31. Marckmann, G. and Verron E. "Comparison of Hyperelastic Models for Rubber-Like Materials" ***Rubber Chemistry and Technology***, Vol. 79, No. 5, (2006), 835-858. doi: 10.5254/1.3547969
32. Joshi, A., Kulkarni, A. and Tadesse, Y. "FludoJelly: Experimental Study on Jellyfish-Like Soft Robot Enabled by Soft Pneumatic Composite (SPC)" ***Robotics***, Vol. 8, No. 4, (2019), 56. doi: 10.3390/robotics8030056
33. Yeoh, O.H. "Some Forms of the Strain Energy Function for Rubber" ***Rubber Chemistry and Technology***, Vol. 66, (1993), 754-771. doi: 10.5254/1.3538343
34. Xavier, M.S., Fleming, A.J. Yong, Y.K. "Finite Element Modeling of Soft Fluidic Actuators: Overview and Recent Developments" ***Advanced Intelligent Systems***, Vol. 3, (2021), 2000187. doi: 10.1002/aisy.202000187
35. Rackl, M. "Material testing and hyperelastic material model curve fitting for Ogden, Polynomial and Yeoh models" In ScilabTEC 2015, Paris, France, (2015) http://dx.doi.org/10.13140/RG.2.2.29552.25600/1
36. Wang, Z., Or, K. and Hirai S. "A dual-mode soft gripper for food packaging" ***Robotics and Autonomous Systems***, Vol. 125, (2020), 103427. doi: 10.1016/j.robot.2020.103427
37. Wang, Z., Kanegae, R. and Hirai S. "Circular Shell Gripper for Handling Food Products" ***Soft Robotics***, Vol. 8, No. 5, (2020), 542-554. doi: 10.1089/soro.2019.0140
38. Cacucciolo, V., Shintake, J. and Shea H. "Delicate yet strong: characterizing the electro-adhesion lifting force with a soft gripper" In 2019 2nd IEEE International Conference on Soft Robotics (RoboSoft) COEX, Seoul, Korea, April 14-18, (2019), 108-113. https://doi.org/10.1109/ROBOSOFT.2019.8722706
39. Li H., Yao, J., Zhou, P., Chen, X., Xu, Y. and Zhao Y. "High-Load Soft Grippers Based on Bionic Winding Effect", ***Soft Robotics***, Vol. 6, No. 2, (2018), 276-288. doi: 10.1089/soro.2018.0024
40. Reddy, A.S., Chembuly, V.V.M.J.S. and Rao, V.V.S.K. "Collision-free Inverse Kinematics of Redundant Manipulator for Agricultural Applications through Optimization Techniques" ***International Journal of Engineering, Transactions A: Basics,*** Vol. 35, No. 7, (2022), 1343-1354. doi: 10.5829/ije.2022.35.07a.13
41. Ishii, K., Matsuo, T., Takemura, Y., Sonoda, T., Nishida, Y., Yasukawa, S. and Fujinaga, T. "Tomato-Harvesting-Robot Competition Towards Smart Agriculture" The 2021 International Conference on Artificial Life and Robotics (ICAROB2021), (2021). https://doi.org/10.5954/ICAROB.2021.PS-1
42. Shahzad, K. and Khan, M.B. "Control of a Robotic Wheel-Chair Prototype for People with Walking Disabilities" ***International Journal of Engineering, Transactions B: Applications***, Vol. 31, No. 5, (2018), 693-698. doi: 10.5829/ije.2018.31.05b.02
43. Sangdani, M.H. and Tavakolpour-Saleh, A.R. "Particle Swarm Optimization Based Parameter Identification Applied to a Target Tracker Robot with Flexible Joint" ***International Journal of Engineering, Transactions B: Aspects***, Vol. 33, No. 9, (2020), 1797-1802. doi: 10.5829/ije.2020.33.09c.14
44. Saadat, M. and Garmsiri, N. "A New Intelligent Approach to Patient-cooperative Control of Rehabilitation Robots" ***International Journal of Engineering, Transactions B: Aspects***, Vol. 27, No. 3, (2014), 467-474. doi: 10.5829/idosi.ije.2014.27.03c.15

## Persian Abstract

**چکیده**

رباتیک نرم با استفاده از محرک‌های شبکه پنوماتیک (Pneu-Net) یک زمینه در حال توسعه است که آینده امیدوارکننده‌ای برای کاربردهای مختلف شامل عملیات ظریف مانند کمک‌های زیست پزشکی دارد. تعامل بین هندسه و عملکرد محرک موضوع مهمی است که توسط بسیاری از محققان در این زمینه مورد بررسی قرار گرفته است. با این حال، در مورد رابطه بین قابلیت چنگ زدن و پارامترهای هندسی محرک‌های نرم تحقیقی وجود ندارد. به ویژه، نیاز به روشن کردن تأثیرات ضخامت دیواره بر نیروی چنگ زدن ایجاد شده وجود دارد. در مطالعه حاضر، یک محرک نرم PneuNet محفظه‌ای نیمه استوانه‌ای به صورت عددی برای ارزیابی اثرات تغییرات فشار و ضخامت دیواره بر ویژگی‌های عملکرد آن مورد بررسی قرار گرفته است. نتایج نشان داد که افزایش ضخامت لایه بازدارنده (RLT) به قابلیت خمشی محرک کمک می کند در حالی که افزایش ضخامت دیواره محفظه آن را کاهش می دهد. بنابراین، حداکثر خمش محرک در ترکیب حداقل ضخامت دیواره و حداکثر RLT به دست می آید. در این پیکربندی‌های هندسی حداکثر خمش، روابط تغییر شکل–فشار از یک تابع سیگموئیدی پیروی می‌کنند و با افزایش ضخامت دیواره و کاهش RLT به سمت خطی شدن گرایش پیدا می‌کنند. نیروی چنگ زدن با افزایش فشار کاری و ضخامت دیواره افزایش نمایی را نشان داد. حداکثر نیروی گرفتن به صورت مکعبی با افزایش ضخامت دیواره در حداکثر فشار کاری مربوطه افزایش یافت که با استفاده از مدل رگرسیون چند جمله‌ای (٪$R^2$ = 99.79) مدل‌سازی شد.